Quasiclassical determination of the in-plane magnetic field phase diagram of superconducting Sr_2RuO_4

R. P. Kaur,[1] D. F. Agterberg,[1] and H. Kusunose[2]
[1]*Department of Physics, University of Wisconsin-Milwaukee, Milwaukee, Wisconsin 53211, USA*
[2]*Department of Physics, Tohoku University, Sendai 980-8578, Japan*
(Received 8 March 2005; revised manuscript received 22 July 2005; published 28 October 2005)

We have carried out a determination of the magnetic field temperature (*H-T*) phase diagram for realistic models of the high-field superconducting state of tetragonal Sr_2RuO_4 with fields oriented in the basal plane. This is done by a variational solution of the Eilenberger equations. This has been carried for spin-triplet gap functions with a $\boldsymbol{d}$ vector along the *c* axis (the chiral *p*-wave state) and with a $\boldsymbol{d}$ vector that can rotate easily in the basal plane. We find that, using gap functions that arise from a combination of nearest- and next-nearest-neighbor interactions, the upper critical field can be approximately isotropic as the field is rotated in the basal plane. For the chiral $\boldsymbol{d}$ vector, we find that this theory generically predicts an additional phase transition in the vortex state. For a narrow range of parameters, the chiral $\boldsymbol{d}$ vector gives rise to a tetracritical point in the *H-T* phase diagram. When this tetracritical point exists, the resulting phase diagram closely resembles the experimentally measured phase diagram for which two transitions are only observed in the high-field regime. For the freely rotating in-plane $\boldsymbol{d}$ vector, we also find that an additional phase transition exists in the vortex phase. However, this phase transition disappears as the in-plane $\boldsymbol{d}$ vector becomes weakly pinned along certain directions in the basal plane.

DOI: 10.1103/PhysRevB.72.144528 PACS number(s): 74.20.−z, 74.25.−q

I. INTRODUCTION

It is widely believed that tetragonal Sr_2RuO_4 (Refs. 1–3) is a spin-triplet chiral *p*-wave superconductor. In particular, a pairing state characterized by a gap function $\boldsymbol{d}=\hat{z}(k_x \pm ik_y)$ best explains existing experimental results. The observation of the appearance of local magnetic moments below the superconducting transition temperature by muon spin-resonance (μSR) measurements of Luke *et al.*[4] can qualitatively be accounted for by the twofold degeneracy of the order parameter (a nondegenerate order parameter cannot give rise to local magnetic moments). The nuclear magnetic resonance[5,6] and spin polarized neutron-scattering measurements[7] carried out for fields applied perpendicular to the fourfold symmetric *c* axis show that the spin susceptibility is unchanged by the normal to superconductor transition. This is naturally explained by $\boldsymbol{d}=\hat{z}(k_x \pm ik_y)$ since the $\boldsymbol{d}$ vector is perpendicular to the magnetic field for which no change of spin susceptibility is expected. Also, the Josephson experiments of Liu *et al.* arguably place the strongest constraint on the orientation of $\boldsymbol{d}$ vector[8,9] and also implies a chiral *p*-wave superconducting state with $\boldsymbol{d}\|\hat{z}$. Finally, the observed field distribution of the vortex lattice for the field along the *c* axis is not consistent with a nondegenerate (single component) order parameter but can be accounted for by the chiral *p*-wave state.[10,11]

These experiments provide a convincing picture in favor of a chiral *p*-wave superconductor. However, there are some experiments that do not directly support this state. In particular, the more recent Knight shift measurements of Murakawa *et al.* have been carried out for the field along the *c* axis.[6] These measurements reveal no change in the spin susceptibility. For this field orientation, this would lead to the conclusion that $\boldsymbol{d}$ vector is in the basal plane, not along the *c* axis as would be the case for the chiral *p*-wave state. The simplest interpretation of this experiment is that the magnetic field is sufficiently strong as to rotate $\boldsymbol{d}$ from $\hat{z}$ to the basal plane. This would imply that the transition temperatures for $\boldsymbol{d}$ in the plane are close but slightly less than that for $\boldsymbol{d}$ along $\hat{z}$. This is possible if spin-orbit coupling is weak. Another explanation for the Knight shift data is that the $\boldsymbol{d}$ vector is in the basal plane, but free to rotate in the plane. This would require all four possible in-plane degrees of freedom to be degenerate (or at least nearly degenerate). If this is the case then for any in-plane field orientation, the $\boldsymbol{d}$ vector will have an in-plane component perpendicular to the field. Consequently, the spin susceptibility will remain unchanged for fields applied in the basal plane as well.

Another difficulty with the chiral *p*-wave state is that, for magnetic fields applied in the basal plane, there are two qualitative predictions for which there is little experimental evidence. These are

(i) the existence of an anisotropy in the upper critical field as the field is rotated perpendicular to the fourfold symmetry axis that *does not vanish as* $T \to T_c$;[12]

(ii) the existence of a phase transition in the vortex state in addition to the usual transitions at H_{c2} and H_{c1}. This additional transition is due to a change in the structure of the order parameter.[13]

The primary goal of this work is to understand if there are microscopic theories of the chiral *p*-wave state that can lead to situations where the above predictions (i) and (ii) do not hold. We find that it is plausible that one of the two predictions does not hold, but it is less likely that both do not hold. Intriguingly, this analysis also points to the possibility of a tetra-critical point in the *H-T* phase diagram. This tetracritical point has features that agree with recent experimental measurements in high magnetic fields.[14] Given the difficulties that the chiral *p*-wave state has explaining the *H-T* phase diagram, we also address the possibility of an in-plane $\boldsymbol{d}$

vector to see if it can account for the observed phase diagram. This follows a discussion of the limited conditions for which an in-plane $\boldsymbol{d}$ vector is consistent with experimental results. We find that an in-plane $\boldsymbol{d}$ vector that is nearly free to rotate in the plane can explain the H-T phase diagram.

The paper begins with an overview of Ginzburg-Landau theory for the chiral p-wave state to provide the origin of the two predictions (i) and (ii) above. Then we discus the role of spin-orbit coupling on the orientation of the $\boldsymbol{d}$ vector. This discussion motivates an examination of the quasiclassical equations in a magnetic field for which more than one irreducible representation is important. The quasiclassical equations are solved using an approximation that is valid in high-field regime for all temperatures. We present the resulting H-T phase diagrams for the chiral p-wave state. Finally, after a discussion of the consistency of an in-plane $\boldsymbol{d}$ vector with existing experimental results, we present results on the H-T phase diagram for this case as well.

II. GINZBURG-LANDAU THEORY

The simplest framework within which the role of magnetic fields on the chiral p-wave state can be understood is the Ginzburg-Landau theory. Here we give a brief overview of this theory to demonstrate the origin of the additional transition and the anisotropy in the upper critical field that we will discuss later within a microscopic theory. The free-energy density for the E_u representation of D_{4h} with a basis $\boldsymbol{\eta}=(\eta_x,\eta_y)$ [this basis has the same rotation properties as (x,y)] is given by[12,15]

$$\begin{aligned} f=&-|\boldsymbol{\eta}|^2+|\boldsymbol{\eta}|^4/2+\beta_2(\eta_x\eta_y^*-\eta_y\eta_x^*)^2/2+\beta_3|\eta_x|^2|\eta_y|^2\\ &+|D_x\eta_x|^2+|D_y\eta_y|^2+\kappa_2(|D_y\eta_x|^2+|D_x\eta_y|^2)\\ &+\kappa_5(|D_z\eta_x|^2+|D_z\eta_y|^2)+\kappa_3[(D_x\eta_x)(D_y\eta_y)^*+\text{H.c.}]\\ &+\kappa_4[(D_y\eta_x)(D_x\eta_y)^*+\text{H.c.}]+\boldsymbol{h}^2/(8\pi), \end{aligned} \tag{1}$$

where $D_j=\nabla_j-(2ie/\hbar c)A_j$, $\boldsymbol{h}=\boldsymbol{\nabla}\times\mathbf{A}$, and $\mathbf{A}$ is the vector potential. There are three possible homogeneous phases:[12,15] (a) $\boldsymbol{\eta}=(1,i)/\sqrt{2}$ ($\beta_2>0$ and $\beta_2>\beta_3/2$), (b) $\boldsymbol{\eta}=(1,0)$ ($\beta_3>0$ and $\beta_2<\beta_3/2$), and (c) $\boldsymbol{\eta}=(1,1)/\sqrt{2}$ ($\beta_3<0$ and $\beta_2<0$). Phase (a) is nodeless (if the Fermi surface has the same topology as a cylinder) and phases (b) and (c) have line nodes. Weak coupling theories give rise to phase (a): the chiral p-wave phase. The application of a magnetic field in the basal plane breaks the degeneracy of the two components η_x and η_y. For the chiral p-wave state, symmetry arguments imply that the vortex lattice phase diagram contains at least two vortex lattice phases for magnetic fields applied along any of the four twofold symmetry axes: {(1,0,0), (0,1,0), (1,1,0), (1,−1,0)}.[13,16] To illustrate the origin of these phase transitions, consider a zero-field ground state $\boldsymbol{\eta}=(1,i)$ and a magnetic field applied along the (1,0,0) direction. Due to the broken tetragonal symmetry, the degeneracy of the $\boldsymbol{\eta}=(1,0)$ and the $\boldsymbol{\eta}=(0,1)$ solutions is removed by the magnetic field. Consequently, only one of these two possibilities will order at the upper critical field. However, if the system is spatially uniform along the magnetic field, then the solution near the upper critical field will exhibit a symmetry that the zero-field solution does not. For our example, this symmetry is either σ_x [if $\boldsymbol{\eta}=(0,1)$ orders at H_{c2}] or $-\sigma_x=U(\pi)\sigma_x$ [if $\boldsymbol{\eta}=(1,0)$ orders at H_{c2}] where $U(\pi)$ is a gauge transformation and σ_x is a reflection through the x axis. The only way this can occur is if there is an additional phase transition as magnetic field is reduced to break this symmetry. The only difference that occurs for the field applied along the (1,1,0) direction is that the solution near the upper critical field will be either $\boldsymbol{\eta}=(1,1)$ or $\boldsymbol{\eta}=(1,-1)$.

Another result of the E_u theory that follows from Eq. (1), originally shown by Gor'kov, is that the upper critical field is anisotropic near T_c.[12] Such an anisotropy, for which $dH_{c2}/dT|_{T=T_c}$ is not equal for (1,0,0) and the (1,1,0) directions, cannot occur for order parameters that have only one complex degree of freedom.[12] The anisotropy in upper critical field near T_c has been calculated from microscopic calculations for the in-plane fields, along the (1,0,0) and (1,1,0) directions, for a gap function of the form $\boldsymbol{d}(\boldsymbol{k})=\hat{\boldsymbol{z}}[\eta_x f_x(\boldsymbol{k})+\eta_y f_y(\boldsymbol{k})]$.[17] These calculations show that anisotropy is generally much larger than that experimentally observed. However, under certain special circumstances, this anisotropy can be small.[17] To examine the lack of anisotropy for the whole temperature range requires a microscopic model that goes beyond the Ginzburg-Landau theory as is done below. Note that previous microscopic studies of the chiral p-wave state for in-plane magnetic fields[18,19] did not reveal the physics discussed here. This was because the order parameter in these works was fixed to have the form $\boldsymbol{\eta}=(1,i)$ for all magnetic fields and temperatures. Such an approximation is valid only for fields much smaller than H_{c2}.

III. SPIN-ORBIT COUPLING AND THE ORIENTATION OF $\boldsymbol{d}$

An important interaction in determining the specific spin-triplet pairing state in Sr_2RuO_4 is spin-orbit coupling. We quantify this in this section. From a symmetry point of view, the superconducting state belongs to one of the odd-parity representations of the tetragonal point group D_{4h}.[12,15] The quasi-two-dimensionality of the Fermi-liquid state in Sr_2RuO_4 makes it reasonable to assume that the momentum dependence of the superconducting state is described by functions $f_x(\boldsymbol{k})$ and $f_y(\boldsymbol{k})$ which obey the same symmetry transformation properties as k_x and k_y, respectively, under rotations of D_{4h} (but otherwise are arbitrary). When there is no spin-orbit coupling, the spin-triplet state has sixfold degeneracy,[20,21] the transition temperature T_c will be same

TABLE I. Gap functions and interaction strengths for the different representations of D_{4h}.

Rep (Γ)	Gap function	Interaction (V_Γ)
A_{1u}	$\hat{x}f_x+\hat{y}f_y$	$g_z-2(g_2+g_3)$
A_{2u}	$\hat{x}f_y-\hat{y}f_x$	$g_z+2(g_2+g_3)$
B_{1u}	$\hat{x}f_x-\hat{y}f_y$	$g_z-2(g_2-g_3)$
B_{2u}	$\hat{x}f_y+\hat{y}f_x$	$g_z+2(g_2-g_3)$
E_u	$\hat{z}(f_x\pm if_y)$	$2g_1-g_z$

for any linear combination for gap functions given in Table I. When spin-orbit coupling is included, the degeneracy of T_c will be lifted. The stable state will either have the $\boldsymbol{d}$ vector along the c axis or be a linear combination of in-plane $\boldsymbol{d}$ vectors.

To quantify the role of spin-orbit coupling, we follow an approach developed by Sigrist *et al.*[22] In particular, the effect of spin-orbit coupling is included through the magnetic susceptibility. The Hamiltonian with a general pairing interaction is

$$\mathcal{H} = \sum_{\boldsymbol{k},s} \epsilon_{\boldsymbol{k}} c^{\dagger}_{\boldsymbol{k}s} c_{-\boldsymbol{k}s} + \frac{1}{2} \sum_{\boldsymbol{k},\boldsymbol{k}'} \sum_{s_1 s_2 s_3 s_4} V_{\boldsymbol{k},\boldsymbol{k}';s_1 s_2 s_3 s_4} c^{\dagger}_{\boldsymbol{k}s_1} c^{\dagger}_{-\boldsymbol{k}s_2} c_{-\boldsymbol{k}'s_3} c_{\boldsymbol{k}'s_4}, \tag{2}$$

where $\epsilon_{\boldsymbol{k}}$ is electron band energy measured from the Fermi energy and $c^{\dagger}_{\boldsymbol{k}s}, c_{\boldsymbol{k}s}$ are the fermion creation and annihilation operators. As a concrete model, we use an effective pairing interaction that is due to spin fluctuations.[22] However, the results that we require later depend solely upon the splitting of the sixfold degeneracy (this can be incorporated in a model independent way within the quasiclassical theory). The effective pairing interaction we use is

$$V_{\boldsymbol{k}\boldsymbol{k}',s_1,s_2,s_3,s_4} = -\frac{I^2}{16} \sum_{\mu,\nu} \{[\chi_{\mu,\nu}(\boldsymbol{k},\boldsymbol{k}') + \chi_{\nu,\mu}(\boldsymbol{k},\boldsymbol{k}')]\sigma^{\mu}_{s_1,s_4}\sigma^{\nu}_{s_2,s_3} - [\chi_{\mu,\nu}(-\boldsymbol{k},\boldsymbol{k}') + \chi_{\nu,\mu}(\boldsymbol{k},-\boldsymbol{k}')]\sigma^{\mu}_{s_2,s_4}\sigma^{\nu}_{s_1,s_3}\}, \tag{3}$$

where I is a coupling constant, and $\chi_{\mu\nu}(\boldsymbol{k},\boldsymbol{k}')$ is the static susceptibility. The phenomenological form of $\chi_{\mu,\nu}(\boldsymbol{k},\boldsymbol{k}')$ in a material of tetragonal symmetry is

$$\chi_{\mu,\nu}(\boldsymbol{k},\boldsymbol{k}') = \begin{pmatrix} g_1(f_x f'_x + f_y f'_y) + g_2(f_x f'_x - f_y f'_y) & g_3(f_x f'_y + f_y f'_x) & 0 \\ g_3(f_x f'_y + f_y f'_x) & g_1(f_x f'_x + f_y f'_y) - g_2(f_x f'_x - f_y f'_y) & 0 \\ 0 & 0 & g_z(f_x f'_x + f_y f'_y) \end{pmatrix}, \tag{4}$$

where g_1, g_2, g_3, and g_z are phenomenological parameters. The self-consistency equation for the $\boldsymbol{d}$ vector with the above interaction can be solved to get the superconducting transition temperature, $k_B T_c = 1.14\omega_c \exp[-16/I^2 N(0) V_\Gamma]$ for the different representations Γ (V_Γ corresponds to the interaction for the representation Γ). These are listed in Table I.

In the limit $g_1 = g_z$ and $g_2 = g_3 = 0$ there is no spin-orbit coupling and all the representations will be degenerate. If there is cylindrical symmetry then $g_2 = g_3$. Notice that this does not imply that that all the in-plane pairing states are degenerate. For this to occur, $g_2 = g_3 = 0$. It is instructive to use results from recent microscopic calculations to gain an insight into the relative size of $\{g_1, g_2, g_3, g_z\}$.[21,23] Both these papers reveal that deviation from the isotropic limit is small, since all the representations have very similar transition temperatures. The results of Ref. 23 correspond to the limit $g_3 = 0$, $g_1 > g_z$, and $|g_1 - g_z| \gg |g_2|$. Based on these results we will assume that $|g_2|, |g_3| \ll |g_1 - g_z|$. The case $g_1 > g_z$ corresponds to the chiral pairing state.[21,22] While the case $g_z > g_1$ and $|g_2|$, $|g_3| \ll |g_1 - g_z|$ corresponds to the nearly degenerate in-plane $\boldsymbol{d}$ vector. We will consider both these cases in the following.

IV. EILENBERGER EQUATIONS FOR THE γ BAND

An important aspect for understanding the superconducting state in Sr_2RuO_4 is the band structure. In particular, the states near the Fermi surface are derived from the Ru t_{2g} orbitals. The degeneracy of these orbitals are split by the tetragonal crystal field into a xy orbital and the degenerate $\{xz, yz\}$ orbitals.[24–27] These two sets of orbitals have a different parity under a mirror reflection through the basal plane. Consequently, to first approximation, the γ sheet of the Fermi surface is comprised of xy Wannier functions, while the $\{\alpha, \beta\}$ sheets of the Fermi surface are comprised of $\{xz, yz\}$ Wannier functions. This leads naturally to orbital dependent superconductivity;[28,29] a theory for the superconducting state that has different gaps on the $\{\alpha, \beta\}$ and γ sheets of the Fermi surface. This theory has experimental support through specific-heat measurements in magnetic fields.[30,31] These measurements indicate that for strong fields applied in the basal plane, superconductivity in the $\{\alpha, \beta\}$ bands is suppressed and the γ band has the dominant superconducting gap. In addition to these measurements, recent theoretical calculations indicate that the ratio of the $\{\alpha, \beta\}$ band gaps to that of the γ band gap is ≈ 0.15 in the high-field limit.[19] Therefore we restrict the following microscopic theory in the high-field regime to a single band theory for the γ band.

Now we will explain briefly the approximate analytic solution of the fundamental quasiclassical equations for a single band within weak-coupling superconductivity under magnetic fields. Our notation and formulation follows that of Ref. 19. The solution can be obtained by the following approximations: (i) the spatial dependence of the internal magnetic field is averaged by B, (ii) the vortex lattice structure is expressed by the Abrikosov lattice, and (iii) the diagonal elements of the Green's function are approximated by the spatial average. In general, a magnetic field will mix different representations of the D_{4h}. Consequently, the $\boldsymbol{d}$ vector will be a linear combination of the functions listed in Table I,

$$\boldsymbol{d}(\boldsymbol{R},\boldsymbol{k}) = d_1(\boldsymbol{R})[\hat{x}f_x(\boldsymbol{k}) + \hat{y}f_y(\boldsymbol{k})] + d_2(\boldsymbol{R})[\hat{x}f_y(\boldsymbol{k}) + \hat{y}f_x(\boldsymbol{k})] + d_3(\boldsymbol{R})[\hat{x}f_x(\boldsymbol{k}) - \hat{y}f_y(\boldsymbol{k})] + d_4(\boldsymbol{R})[\hat{x}f_y(\boldsymbol{k}) - \hat{y}f_x(\boldsymbol{k})] + \hat{z}[\eta_x(\boldsymbol{R})f_x(\boldsymbol{k}) + \eta_y(\boldsymbol{R})f_y(\boldsymbol{k})]; \quad (5)$$

the form of $f_x(\boldsymbol{k})$ and $f_y(\boldsymbol{k})$ is given in next subsection. The approximation (ii) amounts to taking each order-parameter component in the lowest Landau level, so that $\boldsymbol{d}(\boldsymbol{R},\boldsymbol{k}) = \Delta\phi_0(\boldsymbol{R})\tilde{\boldsymbol{d}}(\boldsymbol{k})$, where ϕ_0, the lowest Landau level, is given by

$$\phi_0(\boldsymbol{R}) = \sum_n c_n e^{-ip_n y'} \exp\{-[(x' - \Lambda^2 p_n)/\Lambda]^2/2\}, \quad (6)$$

where $p_n = 2\pi n/\beta$, β being the lattice constant in the y direction, $\Lambda = (2|e|B)^{-1/2}$ is the magnetic length, and the coefficients c_n, which determine the type of vortex lattice, are such that $\langle|\phi_0(\boldsymbol{R})|^2\rangle = 1$, Δ is the magnitude of gap, and $\tilde{\boldsymbol{d}}(\boldsymbol{k})$ defines the angular dependence of the $\boldsymbol{d}$ vector. We have taken anisotropy into account by writing $x = x'/\chi^{1/2}$ and $y = y'\chi^{1/2}$. For a conventional superconductor, even though all approximations mentioned above are valid near H_{c2}, comparisons with reliable numerical calculations suggest that the solution is competent quantitatively in the wide region of the (T,H) phase diagram except in very low T and H regions.[32] For further details we recommend the reader to refer to the literature.[32–36] In principle, we should consider higher Landau level solutions in this problem. However, within Ginzburg-Landau theory our solution is exact in the high-field limit provided the magnetic field is in the basal plane. This indicates that it is reasonable to keep only the lowest Landau level (for the field along the c axis, other Landau levels must be included[13]). The expression for the free energy measured relative to the normal-state energy,[32] which is given for strongly type-II superconductors, $B \simeq H$, in the clean limit is

$$\Omega_{SN}/N_0 = \ln\left(\frac{T}{T_c^z}\right)(|\eta_x|^2 + |\eta_y|^2) + \sum_{\Gamma=1}^{4} |d_\Gamma|^2 \ln\left(\frac{T}{T_c^\Gamma}\right) + 2\pi T \sum_{n=0}^{\infty}\left(\frac{\Delta^2}{\omega_n} - \langle I\rangle\right), \quad (7)$$

where N_0 is the total density of states (DOS) in the normal state, and $\omega_n = (2n+1)\pi T$ is the Fermionic Matsubara frequency. Equation (7) generalizes the corresponding expressions in earlier works[32–36] by including more than one irreducible representation. The function I is given by

$$I = \frac{2g}{1+g}\sqrt{\pi}\left(\frac{2\Lambda}{\tilde{v}_\perp(\hat{\boldsymbol{k}})}\right)\Delta^2|\varphi(\hat{\boldsymbol{k}})|^2 W(iu_n), \quad (8)$$

with

$$g = \left[1 + \frac{\sqrt{\pi}}{i}\left(\frac{2\Lambda}{\tilde{v}_\perp(\hat{\boldsymbol{k}})}\right)^2 \Delta^2|\varphi(\hat{\boldsymbol{k}})|^2 W'(iu_n),\right]^{-1/2}, \quad (9)$$

where $u_n = 2\Lambda\omega_n/\tilde{v}_\perp(\boldsymbol{k})$, $W(z) = e^{-z^2}\,\mathrm{erfc}(-iz)$ is the Faddeeva function, and $|\varphi(\hat{\boldsymbol{k}})|^2 = \tilde{\mathbf{d}}(\boldsymbol{k})\cdot\tilde{\mathbf{d}}^*(\boldsymbol{k})$. Here $\tilde{v}_\perp(\hat{\boldsymbol{k}})$ is the component of $\boldsymbol{v}$ perpendicular to the field, which for an in-plane field of the form $\boldsymbol{H} = H(\cos\phi_h, \sin\phi_h, 0)$ is given as

$$\tilde{v}_\perp^2(\hat{\boldsymbol{k}}) = \chi^{-1/2}v_z^2 + \chi^{1/2}v_F^2\sin^2(\phi - \phi_h), \quad (10)$$

where $\chi = \tilde{\chi}v_F/v_c$ is an anisotropy parameter (we let $\tilde{\chi}$ be arbitrary). We have taken $v_z(k) = v_c\,\mathrm{sgn}(k_z)$. All fields are measured in units $2\pi^2T_c^2/(ev_Fv_c)$ and $\hbar$ and k_B are both 1. We will use this formalism to examine the in-plane magnetic field phase diagram for the chiral p-wave state and the nearly degenerate in-plane $\boldsymbol{d}$ vector separately.

A. Momentum dependence of the gap function

To complete the description of the superconducting state, we must specify the functions $f_i(\boldsymbol{k})$ $(i = \{x,y\})$. The most general gap function consistent with translational invariance and with the appropriate rotational properties of D_{4h} is

$$f_i(\boldsymbol{k}) = \sum_{n=1,m=0}^{\infty} c_{n,m}\sin(nk_i)\cos(mk_j), \quad i,j = x,y, \quad i \neq j, \quad (11)$$

where $c_{n,m}$ are complex coefficients, k_i in units π/a, and a is the lattice spacing. Here $n=1$, $m=0$ represents a Cooper pair formed by nearest-neighbor (NN) interactions and $n=1$, $m=1$ to a Cooper pair formed from next-nearest-neighbor (NNN) interactions. In general, increasing m,n corresponds to forming Cooper pairs from interactions between increasing number of neighbors. We will restrict ourselves here to NN and NNN pairing interactions. This has some support from microscopic calculations. In particular, the theory for NN interactions was originally proposed by Miyake and Narikiyo[37] and was also examined by Nomura and Yamada.[38] Cooper pairs for which NN interactions are not important but which have a substantial contribution from NNN interactions have been proposed recently by Arita *et al.*[39] with the assumption of large on-site and nearest-neighbor Coulomb interactions. In particular, the latter paper proposes a gap function of the form $\boldsymbol{d} = \hat{\boldsymbol{z}}[\sin(k_x + k_y) - i\sin(k_x - k_y)] = \hat{\boldsymbol{z}}\sqrt{2}e^{-i\pi/4}[\sin k_x\cos k_y + i\sin k_y\cos k_x]$. We take Cooper pairs to be formed by NN and NNN interactions and take the form of f_x to be $f_x = \sin(k_x)[1 + \epsilon\cos(k_y)]$. We keep the parameter ϵ to be arbitrary and allow it to vary. We take the Fermi surface to be cylindrical with $(k_x,k_y) = \pi R(\cos\phi, \sin\phi)$ where $R = 0.9$ approximates the Fermi surface of the gamma band (in the third subsection of next section we will take $R = 0.79$ for reasons that will be apparent).

V. CHIRAL p-WAVE STATE

For the chiral p-wave state, we use $\boldsymbol{d}(\boldsymbol{k},\boldsymbol{R}) = \hat{\boldsymbol{z}}\Delta\phi_0(\boldsymbol{R})\varphi(\hat{\boldsymbol{k}})$ with

$$\varphi(\hat{\boldsymbol{k}}) = [\cos\theta f_x(\boldsymbol{k}) + \sin\theta e^{i\zeta}f_y(\boldsymbol{k})] \quad (12)$$

(not normalized for notational simplicity). For this gap function, the Ginzburg-Landau order parameter takes the specific form $\boldsymbol{\eta}(\boldsymbol{R}) = \Delta\phi_0(\boldsymbol{R})(\cos\theta, e^{i\zeta}\sin\theta)$.

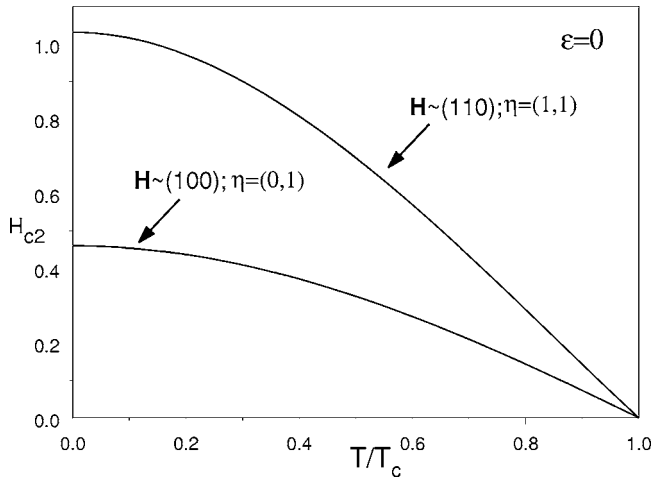

FIG. 1. Upper critical fields for $\epsilon=0$ for the fields along the (1,0,0) and (1,1,0) directions. The field in units $2\pi^2T_c^2/(ev_Fv_c)$.

A. Upper critical field

The anisotropy in upper critical field for (1,0,0) and (1,1,0) directions is a generic feature of the E_u theory. Since experimentally it has been observed that the upper critical field is relatively isotropic for in-plane fields,[14] we ask if it is possible to reproduce this. The only free parameter in the theory is ϵ which describes the anisotropy in the gap function. Surprisingly, we have found that it is possible for $\epsilon=10$. The upper critical field for the field in the (1,1,0) and the (1,0,0) directions for the three values of ϵ; $\epsilon=0$, $\epsilon=\infty$, and $\epsilon=10$ for the chiral superconducting state has been shown in Figs. 1–3. In these figures we also show the stable solutions for the order parameter at H_{c2}. For a field along the (1,0,0) direction, the possible stable solutions are $\boldsymbol{\eta}=(1,0)$ or $\boldsymbol{\eta}=(0,1)$. For a field along the (1,1,0) direction, the possible stable solutions are $\boldsymbol{\eta}=(1,1)$ or $\boldsymbol{\eta}=(1,-1)$.

B. Phase diagram

Another generic feature of the E_u theory is that multiple vortex phases exist for in-plane fields. For a field along the

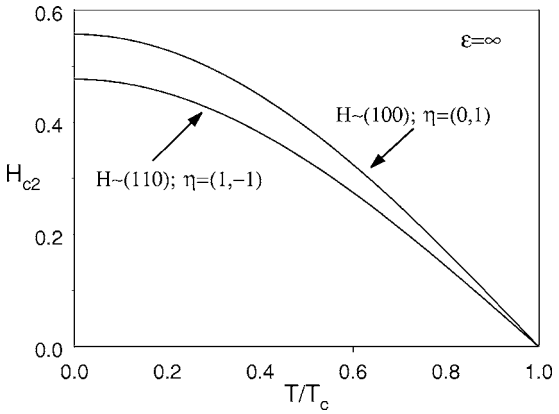

FIG. 2. Upper critical fields for $\epsilon=\infty$ and for the fields along the (1,0,0) and (1,1,0) directions.

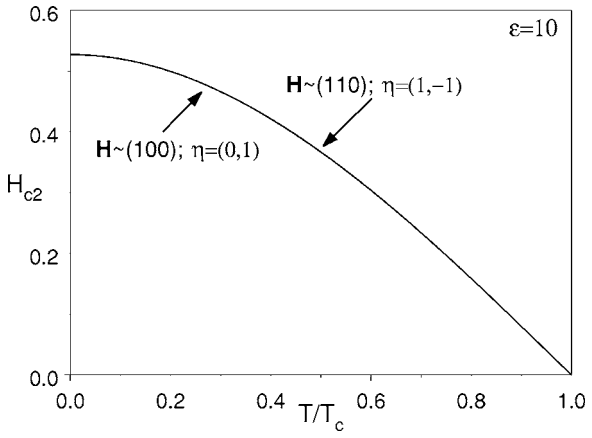

FIG. 3. Upper critical fields for $\epsilon=10$ and for the fields along the (1,0,0) and (1,1,0) directions. The two upper critical fields almost identical.

(1,0,0) direction, the solution near H_{c2} is $\boldsymbol{\eta}=(0,1)$ (for the three values of ϵ discussed above this was the case) then as field is reduced for fixed temperature, a second transition occurs at H_2 for which the $\boldsymbol{\eta}=(1,0)$ component becomes nonzero. Such phase transitions have only been examined within Ginzburg-Landau theory.[28,40] The Eilenberger equations discussed above allow for the examination of this phase transition throughout the entire H-T phase diagram. Here, we apply this approach to the $\epsilon=10$ gap function for a (1,0,0) field direction; the resulting phase diagram is shown in Fig. 4.

The specific heat as a function of temperature is also shown in Fig. 5 for $H/H_{c2}^0=0.21$. This plot clearly shows a second transition in the specific heat. Such a second transition has not been seen in specific-heat measurements. This represents a difficulty for the E_u theory. In general, we have not been able to find a microscopic theory that can account for both the lack of anisotropy in the upper critical field and the lack of the second transition. It is possible that experiments have not seen the predicted specific heat jumps due to the broadening associated with fluctuations in the vortex

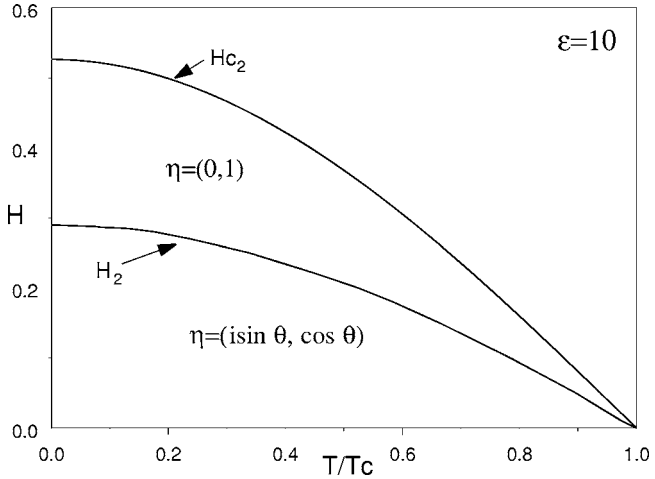

FIG. 4. Phase boundaries for $\epsilon=10$ and for the field along the (100) direction.

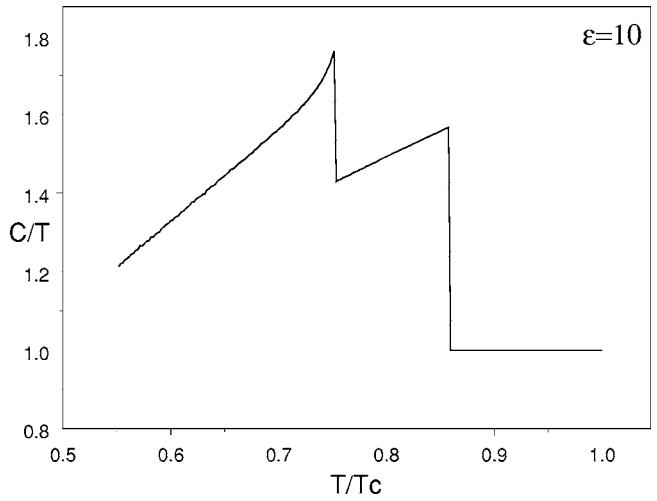

FIG. 5. Specific heat as a function of temperature for a fixed field $H/H_{c2}^{0}=0.21$ and for $\epsilon=10$.

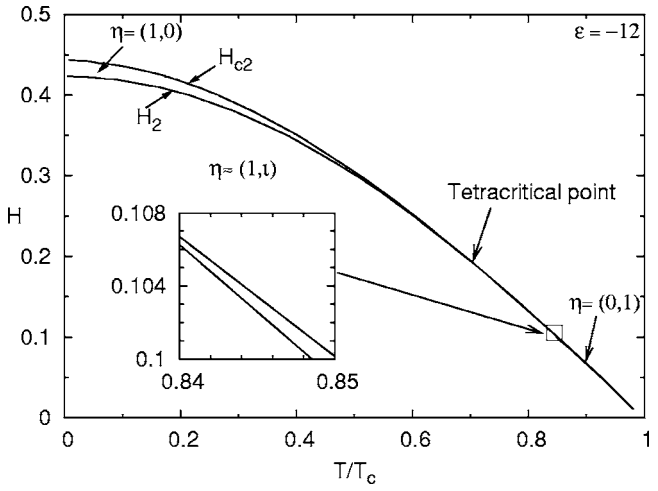

FIG. 6. Phase diagram showing a tetracritical point. Between T_c and the tetracritical temperature there are two phase transitions, shown in the inset, that are difficult to distinguish from each other.

phase, or due to sample inhomogeneities. In the case of UPt_3, for which multiple phase transitions in the vortex phase have been observed, the entire phase diagram was found through ultrasound measurements.[41] Specific-heat measurements mapped out some portions of the phase diagram[42] but they did not show clear anomalies throughout the entire phase diagram.[43] Therefore it would be useful to look for such transitions in the phase diagram for Sr_2RuO_4 with other probes such as ultrasound.

C. Tetracritical point

While there has been no evidence of multiple superconducting transitions in the low-field regime, two superconducting transitions have been observed in the high-field range.[14,44] In one aspect these transitions are natural candidates for two transitions discussed above. In particular, the vanishing of the second transition (which does not occur at H_{c2}) as the field is rotated away from the in-plane direction is consistent with the above predictions. However, the second transition is only observed for $T/T_c<0.1$ and appears to intersect the upper critical field line. This is inconsistent with the above prediction which predicts that this transition should exist for all temperatures. Here we explore a possible explanation for this transition that is based on results of the Eilenberger equations.

We have found that for small parameter ranges in the model described above, it is possible that the solution for the order parameter at the upper critical field *changes* as a function of temperature. In particular for a field along the (1,0,0) direction, the low-temperature solution (at H_{c2}) is $\boldsymbol{\eta}=(1,0)$ and there is a transition as temperature is reduced so that the solution at H_{c2} becomes $\boldsymbol{\eta}=(0,1)$. The phase diagram that emerges bears a striking similarity to the observed results.

In Figs. 6 and 7, we show the phase diagram and specific-heat calculations for $R=0.79$ and $\epsilon=-12$. Note that a negative ϵ corresponds to a repulsive interaction between Cooper pairs formed from nearest and Cooper pairs formed from next-nearest neighbors. This theory would still require the existence of two transitions up to $T=T_c$. However, as this phase diagram shows, the two transition lines between T_c and the temperature of the tetracritical point are very close to each other and will be very difficult to observe experimentally.

While this phase diagram agrees with that observed experimentally for a field along the (1,0,0) direction, this choice of parameters also exhibits a moderate ≈15% anisotropy of the in-plane upper critical field. Furthermore, for the field along the (1,1,0) direction the phase diagram resembles that of Fig. 4 (there is no tetracritical point). Therefore these results can only be taken as suggestive since this set of parameters cannot account for all observed features. It is possible that the gap on the $\{\alpha,\beta\}$ bands may improve the agreement between theory and experiment. It appears that at low fields these gaps cannot be neglected[19] and the suppression of these gaps relative to that of the γ may provide a more robust mechanism for the appearance of a tetracritical point in the relatively low-field regime. This can occur if these

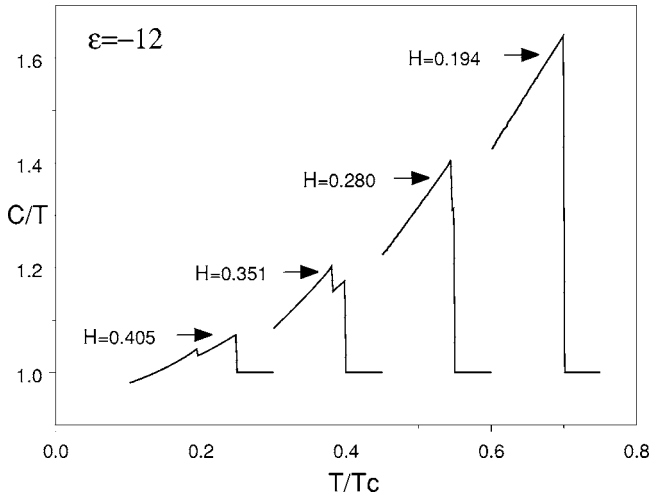

FIG. 7. Specific heat as a function of temperature for fixed magnetic fields.

bands prefer orthogonal order parameter solutions at H_{c2}, as was often the case for calculations for different E_u gap functions in Ref. 17. A second possible explanation for both the observed lack of anisotropy and the existence of a tetracritical point is that the parameter ϵ may not be constant for all temperatures and magnetic fields as we have used here. A complete description would require an effective two-gap theory for which ϵ is determined self-consistently. In such a theory, ϵ can develop a temperature and magnetic field dependence (though in many circumstances, ϵ will be approximately constant). A complete analysis of this would require a detailed knowledge of the microscopic interactions giving rise to superconductivity. This is beyond the scope of this paper.

VI. NEARLY DEGENERATE IN PLANE *d* VECTOR

The chiral *p*-wave state has difficulties explaining both the observed absence of anisotropy in H_{c2} and the absence of additional phase transitions in the vortex phase. For this reason we also consider the nearly degenerate in-plane $\boldsymbol{d}$ vector. Initially, we consider under what circumstances the nearly degenerate $\boldsymbol{d}$ vector is consistent with other experiments (Knight shift, μSR, vortex lattice structure, and Josephson experiments). Then we examine the specific heat as a function of magnetic field in the vortex state and show that the second anomaly is rapidly suppressed by the breaking of the degeneracy of the four components of the in-plane $\boldsymbol{d}$ vector.

Knight-shift measurements can be naturally accounted for by an in-plane $\boldsymbol{d}$ vector. The most recent observation is that for magnetic fields along the *c* axis there is no change in the spin susceptibility as temperature is reduced.[6] The simplest interpretation of this result is that the $\boldsymbol{d}$ vector is in the basal plane. The earlier observation that the spin susceptibility is unchanged for in-plane magnetic fields would require that the $\boldsymbol{d}$ vector is free to rotate in the basal plane. This implies that all the in-plane $\boldsymbol{d}$ vector states are degenerate or nearly degenerate. The observed square vortex lattice for the field along the *c* axis is also consistent with a degenerate in-plane $\boldsymbol{d}$ vector. This will follow from a Ginzburg-Landau analysis, where it can be shown that free energy for the degenerate in-plane $\boldsymbol{d}$ vector has equilibrium solutions with the same properties as those of the Ginzburg-Landau theory for the chiral *p*-wave state.

The muon spin relaxation (μSR) measurements of Luke *et al.*[4] have found an increased spin-relaxation rate in the superconducting state with zero applied magnetic field. This has commonly been interpreted as evidence for a superconductor that breaks time-reversal symmetry in the bulk. However, any bulk internal magnetic field must be screened due to the Meissner effect. Consequently, μSR only probes internal magnetic fields due to inhomogeneities such as impurities or domain walls between degenerate superconducting states. It has been shown that a superconducting state that does not break time-reversal symmetry in the bulk can still give rise to local internal fields.[15] The important condition for such internal magnetic fields to exist is that the superconducting order parameter has more than one degree of freedom. This distinction is emphasized here because for nearly degenerate in-plane $\boldsymbol{d}$ vectors, the bulk superconducting state in zero applied field does not break time-reversal symmetry. This does not imply that such a state is inconsistent with μSR measurements. However, it does require that the different in-plane $\boldsymbol{d}$-vector representations are nearly degenerate (the different T_c values must lie close to each other).

The most difficult experiments to explain with an in-plane $\boldsymbol{d}$ vector are the Josephson experiments. The most recent of these has found that for Sr_2RuO_4-$Au_{0.5}In_{0.5}$ superconducting quantum interference device (SQUID), there is a π phase difference in the Josephson current when the two junctions have opposite normals.[8] While this is generally expected for a *p*-wave superconductor, it cannot be explained by an in-plane $\boldsymbol{d}$ vector. Such a $\boldsymbol{d}$ vector does not allow for a Josephson current between an odd-parity superconductor and an isotropic (*s*-wave) superconductor when the junction has a normal perpendicular to the Sr_2RuO_4 *c* axis. The existence of such a Josephson current implies a $\boldsymbol{d}$ vector aligned along the *c* axis. An explanation of such a Josephson current within an in-plane $\boldsymbol{d}$-vector approach would therefore require that at an interface, the $\boldsymbol{d}$ vector is along the *c* axis and in the bulk it is in-plane. A similar scenario has been proposed by Bahcall in the context of the cuprate superconductors (in this case, the order parameter near the interface is *s*-wave and becomes *d*-wave in the bulk).[45] In support of such a picture, the $\boldsymbol{d}$ vector is almost certainly along the *c* axis for an interface with a normal perpendicular to the *c* axis. This is a natural consequence of a stronger spin-orbit coupling at the interface than in the bulk (spin-orbit coupling is governed by the gradient of the single-particle potential). It is the spin-orbit coupling that governs the orientation of the $\boldsymbol{d}$ vector. A Rashba spin-orbit coupling of the form $\alpha_R \hat{n}\cdot\boldsymbol{k}\times\boldsymbol{S}(k)$ (where $\hat{n}$ is the interface normal, $\boldsymbol{k}$ is the fermion wave number, $\boldsymbol{S}(k)$ is the fermion spin, and α_R is a coupling constant) would give a $\boldsymbol{d}$ with a component along the *c* axis if $\hat{n}$ lies perpendicular to the *c* axis.[46] If the bulk $\boldsymbol{d}$ vector is in-plane and the $\boldsymbol{d}$ vector lies along the *c* axis near the interface, then an analysis following that of Bahcall would imply that the π SQUID experiment of Nelson *et al.* should sometimes see a π phase shift and sometimes no phase shift. Nelson's data indicate that there is always a π phase shift. However, given that data on only three samples are presented, it may be prudent to await further results before ruling out an in-plane $\boldsymbol{d}$ vector in the bulk on the basis of these experiments.

The general form for an in-plane $\boldsymbol{d}$ vector will be a linear combination of four different in-plane representations listed in Table I,

$$\boldsymbol{d}(\boldsymbol{R},\boldsymbol{k}) = d_1(\boldsymbol{R})[\hat{x}f_x(\boldsymbol{k}) + \hat{y}f_y(\boldsymbol{k})] + d_2(\boldsymbol{R})[\hat{x}f_y(\boldsymbol{k}) + \hat{y}f_x(\boldsymbol{k})] + d_3(\boldsymbol{R})[\hat{x}f_x(\boldsymbol{k}) - \hat{y}f_y(\boldsymbol{k})] + d_4(\boldsymbol{R})[\hat{x}f_y(\boldsymbol{k}) - \hat{y}f_x(\boldsymbol{k})]. \tag{13}$$

We parametrize $[d_1(\boldsymbol{R}),d_2(\boldsymbol{R}),d_3(\boldsymbol{R}),d_4(\boldsymbol{R})]$ as $\Delta\phi_0(\boldsymbol{R})(\cos\psi\cos\theta, \sin\psi\sin\phi, \cos\psi\sin\theta, \sin\psi\cos\phi)$ so that the $\boldsymbol{d}$ vector can be written as

$$\boldsymbol{d}(\boldsymbol{R},\boldsymbol{k}) = \Delta(\boldsymbol{R})[\hat{x}\varphi_x(\boldsymbol{k}) + \hat{y}\varphi_y(\boldsymbol{k})], \tag{14}$$

with

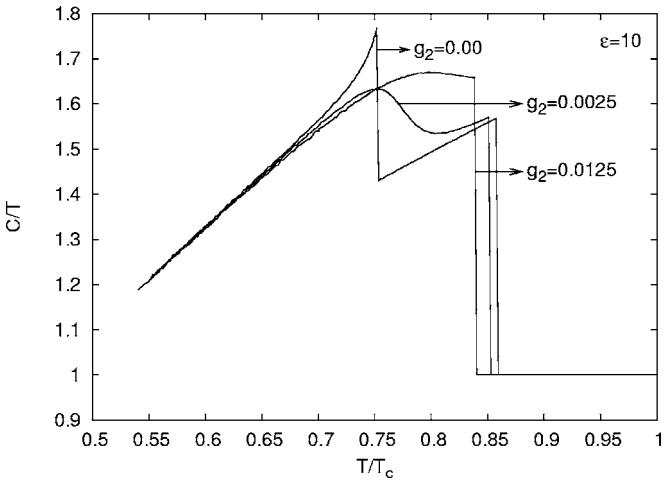

FIG. 8. Specific heat for $\epsilon=10$ for the field along the (1,0,0) direction, with fixed $H/H_{c2}^{0}=0.21$ for different values of g_2 (which is measured here in units g_z).

$$\varphi_x(\hat{\boldsymbol{k}}) = \cos\psi(\cos\theta + \sin\theta) f_x(\boldsymbol{k}) + \sin\psi(\sin\phi + \cos\phi) f_y(\boldsymbol{k})$$

and

$$\varphi_y(\hat{\boldsymbol{k}}) = \cos\psi(\cos\theta - \sin\theta) f_y(\boldsymbol{k}) + \sin\psi(\sin\phi - \cos\phi) f_x(\boldsymbol{k}).$$

With these definitions $|\varphi(\hat{\boldsymbol{k}})|^2 = |\varphi_x(\hat{\boldsymbol{k}})|^2 + |\varphi_y(\hat{\boldsymbol{k}})|^2$.

Prior to presenting the results for the nearly degenerate in-plane $\boldsymbol{d}$ vector, we briefly give the results for the degenerate in-plane $\boldsymbol{d}$ vector. This corresponds to the situation that $g_2=g_3=0$ in Table I. In zero applied field there are many degenerate solutions for this case. In particular, all the solutions in Table I and the solutions $\boldsymbol{d}(\boldsymbol{k})=\hat{e}(k_x \pm ik_y)$, where $\hat{e}$ is any unit vector in the basal plane, are all degenerate ground-state solutions.[20] If a magnetic field is applied along any of the twofold symmetry axes, then there will be two transitions as field is reduced (as there was in the chiral p-wave case). Unlike the chiral p-wave case the second transition can occur in two ways. To illustrate this, consider an applied field along (0, 1, 0) direction, the high-field state (the state corresponding to the transition from normal state to superconducting state) will be either $\hat{x}k_x$ or $\hat{x}k_y$(it has been assumed here that the $\boldsymbol{d}$ vector prefers to be perpendicular to the magnetic field). Consider $\hat{x}k_y$ to be concrete. The second transition will appear as magnetic field is reduced for fixed temperature. The second transition exists because of the appearance of either a $\hat{x}k_x$ component [the corresponding zero-field ground state will be $\hat{x}(k_x \pm ik_y)$]; or a $\hat{y}k_x$ component (the corresponding zero-field ground state will then be $\hat{x}k_y \pm \hat{y}k_x$). Strictly speaking, the latter transition will be energetically less favorable because the $\boldsymbol{d}$ vector is not perpendicular to the magnetic field. However, it is the latter transition that will play a more important role when the degeneracy between the four in-plane $\boldsymbol{d}$ vectors is broken. In this case the solutions at zero field belong to a single irreducible representation while the other zero-field solutions $\hat{x}(k_x \pm ik_y)$ belong to a mixture of more than one irreducible representation.

In Fig. 8, we show the specific heat as a function of temperature for different values of g_2 (we have set $g_2=g_3$ in the following) with fixed magnetic field, $H/H_{c2}^{0}=0.21$ along (0,1,0) direction for $\epsilon=10$ and $R=0.9$. For $g_2=0$, as discussed above, the second transition will exist and there are two specific-heat anomalies. The second transition is removed by a finite value of g_2/g_z. The key result is that the anomaly for the second transition is very quickly suppressed by a nonzero g_2/g_z. Note that the anisotropy in H_{c2} will still be small for small values of g_2. Consequently, a nearly degenerate in-plane $\boldsymbol{d}$ vector can explain the existing experimental observations on the H-T phase diagram.

The nearly degenerate in-plane $\boldsymbol{d}$ vector can account for the in-plane phase diagram and can qualitatively account for other key experimental results in Sr_2RuO_4. However, prior to carrying out further calculations with this state we note that it should be possible to rule such a state out experimentally in the near future. In particular, there are two predictions that can be made about an in-plane $\boldsymbol{d}$ vector. The first has been mentioned above: further π SQUID experiments should reveal the existence of squids with no phase shift as well as squids with π phase shifts. Also, further Knight-shift experiments should show a suppression in the spin susceptibility for low enough in-plane magnetic fields. This will occur because in zero field the $\boldsymbol{d}$ vector will correspond to a single-component irreducible representation once g_2 and g_3 are nonzero and therefore contain a component that is along the applied field.

VII. CONCLUSIONS

To address an apparent conflict between theoretical predictions of chiral p-wave (the E_u representation) theories of the superconducting state in Sr_2RuO_4 and the lack of corresponding observations, we have carried out quasiclassical calculations of the superconducting phase diagram for in-plane magnetic fields. This has been done for both the chiral p-wave state and for the nearly degenerate in-plane $\boldsymbol{d}$ vector. For a gap function with momentum dependence due to a combination of nearest- and next-nearest-neighbor interactions defined on the γ band, we find that a small anisotropy in the upper critical field as the field is rotated in plane is possible. However, the same gap functions give rise to an additional phase transition in the vortex state which has not been observed experimentally. For a narrow range of parameters, the theory gives rise to a tetracritical point in the H-T phase diagram. When this tetracritical point exists, the resulting phase diagram closely resembles the experimentally measured phase diagram for which two transitions are only observed in the high-field regime. We have also argued that an in-plane $\boldsymbol{d}$ vector that can easily rotate in the basal plane is consistent with existing experimental results.

ACKNOWLEDGMENTS

We thank Manfred Sigrist for very useful discussions. D.F.A. and R.P.K. were supported by National Science Foundation Grant No. DMR-0381665 and the American Chemical Society Petroleum Research Fund. This work was also supported by the Swiss National Science Foundation.

[1] Y. Maeno, H. Hashimoto, K. Yoshida, S. Nishizaki, T. Fujita, J. G. Bednorz, and F. Lichtenberg, Nature (London) **372**, 532 (1994).
[2] Y. Maeno, T. M. Rice, and M. Sigrist, Phys. Today **54** (1), 42 (2001).
[3] A. P. Makenzie and Y. Maeno, Rev. Mod. Phys. **75**, 657 (2003).
[4] G. M. Luke, Y. Fudamoto, K. M. Kojima, M. I. Larkin, J. Merrin, B. Nachumi, Y. J. Uemura, Y. Maeno, Z. Q. Mao, Y. Mori, H. Nakamura, and M. Sigrist, Nature (London) **394**, 558 (1998).
[5] K. Ishida, H. Mukuda, Y. Kitaoka, K. Asayama, Z. Q. Mao, Y. Mori, and Y. Maeno, Nature (London) **96**, 658 (1998).
[6] H. Murakawa, K. Ishida, K. Kitagawa, Z. Q. Mao, and Y. Maeno, Phys. Rev. Lett. **93**, 167004 (2004).
[7] J. A. Duffy, S. M. Hayden, Y. Maeno, Z. Mao, J. Kulda, and G. J. McIntyre, Phys. Rev. Lett. **85**, 5412 (2000).
[8] K. D. Nelson, Z. Q. Mao, Y. Maeno, and Y. Liu, Science **306**, 1151 (2004).
[9] R. Jin, Y. Liu, Z. Mao, and Y. Maeno, Europhys. Lett. **51**, 341 (2000).
[10] T. M. Riseman, P. G. Kealey, E. M. Forgan, A. P. Mackenzie, L. M. Galvin, A. W. Tyler, S. L. Lee, C. Ager, D. M. Paul, C. M. Aegerter, R. Cubitt, Z. Q. Mao, T. Akima, and Y. Maeno, Nature (London) **396**, 242 (1998).
[11] P. G. Kealey, T. M. Riseman, E. M. Forgan, L. M. Galvin, A. P. Mackenzie, S. L. Lee, D. M. Paul, R. Cubitt, D. F. Agterberg, R. Heeb, Z. Q. Mao, and Y. Maeno, Phys. Rev. Lett. **84**, 6094 (2000).
[12] L. P. Gor'kov, Sov. Sci. Rev., Sect. A **9**, 1 (1987).
[13] D. F. Agterberg, Phys. Rev. Lett. **80**, 5184 (1998).
[14] Z. Q. Mao, Y. Maeno, S. Nishizaki, T. Akima, and T. Ishiguro, Phys. Rev. Lett. **84**, 991 (2000).
[15] M. Sigrist and K. Ueda, Rev. Mod. Phys. **63**, 239 (1991).
[16] D. F. Agterberg, R. Heeb, P. G. Kealey, T. M. Riseman, E. M. Forgan, A. P. Mackenzie, L. M. Galvin, R. S. Perry, S. L. Lee, D. M. Paul, R. Cubitt, Z. Q. Mao, S. Akima, and Y. Maeno, Physica C **341**, 1643 (2000).
[17] D. F. Agterberg, Phys. Rev. B **64**, 052502 (2001).
[18] M. Udagawa, Y. Yanase, and M. Ogata, Phys. Rev. B **70**, 184515 (2004).
[19] H. Kusunose, J. Phys. Soc. Jpn. **73**, 2512 (2004).
[20] T. M. Rice and M. Sigrist, J. Phys.: Condens. Matter **7**, L643 (1995).
[21] K. K. Ng and M. Sigrist, Europhys. Lett. **49**, 473 (2000).
[22] M. Sigrist, D. F. Agterberg, A. Furusaki, C. Honerkamp, K. K. Ng, T. M. Rice, and M. E. Zhitomirsky, Physica C **317**, 134 (1999).
[23] Y. Yanase and M. Ogata, J. Phys. Soc. Jpn. **72**, 673 (2003).
[24] T. Oguchi, Phys. Rev. B **51**, 1385 (1995).
[25] D. J. Singh, Phys. Rev. B **52**, 1358 (1995).
[26] A. P. Mackenzie, S. R. Julian, A. J. Diver, G. J. McMullan, M. P. Ray, G. G. Lonzarich, Y. Maeno, S. Nishizaki, and T. Fujita, Phys. Rev. Lett. **76**, 3786 (1996).
[27] C. Bergemann, S. R. Julian, A. P. Mackenzie, S. Nishizaki, and Y. Maeno, Phys. Rev. Lett. **84**, 2662 (2000).
[28] D. F. Agterberg, T. M. Rice, and M. Sigrist, Phys. Rev. Lett. **78**, 3374 (1997).
[29] M. E. Zhitomirsky and T. M. Rice, Phys. Rev. Lett. **87**, 057001 (2001).
[30] K. Deguchi, Z. Q. Mao, H. Yaguchi, and Y. Maeno, Phys. Rev. Lett. **92**, 047002 (2004).
[31] K. Deguchi, Z. Q. Mao, and Y. Maeno, J. Phys. Soc. Jpn. **73**, 1313 (2004).
[32] H. Kusunose, Phys. Rev. B **70**, 054509 (2004).
[33] U. Brandt, W. Pesch, and L. Tewordt, Z. Phys. **201**, 209 (1967).
[34] W. Pesch, Z. Phys. B **21**, 263 (1975).
[35] A. Houghton and I. Vekhter, Phys. Rev. B **57**, 10831 (1998).
[36] T. Dahm, S. Graser, C. Iniotakis, and N. Schopohl, Phys. Rev. B **66**, 144515 (2002).
[37] K. Miyake and O. Narikiyo, Phys. Rev. Lett. **83**, 1423 (1999).
[38] T. Nomura and K. Yamada, J. Phys. Soc. Jpn. **69**, 3678 (2000).
[39] R. Arita, S. Onari, K. Kuroki, and H. Aoki, Phys. Rev. Lett. **92**, 247006 (2004).
[40] T. Kita, Phys. Rev. Lett. **83**, 1846 (1999).
[41] S. Adenwalla, S. W. Lin, Q. Z. Ran, Z. Zhao, J. B. Ketterson, J. A. Sauls, L. Taillefer, D. G. Hinks, M. Levy, and B. K. Sarma, Phys. Rev. Lett. **65**, 2298 (1990).
[42] R. A. Fisher, S. Kim, B. F. Woodfield, N. E. Phillips, L. Taillefer, K. Hasselbach, J. Flouquet, A. L. Giorgi, and J. L. Smith, Phys. Rev. Lett. **62**, 1411 (1989).
[43] A. P. Ramirez, N. Stucheli, and E. Bucher, Phys. Rev. Lett. **74**, 1218 (1995).
[44] Z. Q. Mao, T. Akima, T. Ando, and Y. Maeno, Physica B **284**, 541 (2000).
[45] S. R. Bahcall, Phys. Rev. Lett. **76**, 3634 (1996).
[46] P. A. Frigeri, D. F. Agterberg, A. Koga, and M. Sigrist, Phys. Rev. Lett. **92**, 097001 (2004).